An *In vivo* Platform for Translational Drug Development in Pancreatic Cancer

Belen Rubio-Viqueira,[1] Antonio Jimeno,[1] George Cusatis,[1] Xianfeng Zhang,[1] Christine Iacobuzio-Donahue,[2] Collins Karikari,[2] Chanjusn Shi,[2] Kathleen Danenberg,[4] Peter V. Danenberg,[6] Hidekazu Kuramochi,[6] Koji Tanaka,[6] Sharat Singh,[5] Hossein Salimi-Moosavi,[5] Nadia Bouraoud,[1] Maria L. Amador,[1] Soner Altiok,[2] Piotr Kulesza,[2] Charles Yeo,[3] Wells Messersmith,[1] James Eshleman,[2] Ralph H. Hruban,[2] Anirban Maitra,[2] and Manuel Hidalgo[1]

Abstract Effective development of targeted anticancer agents includes the definition of the optimal biological dose and biomarkers of drug activity. Currently available preclinical models are not optimal to this end. We aimed at generating a model for translational drug development using pancreatic cancer as a prototype. Resected pancreatic cancers from 14 patients were xenografted and expanded in successive groups of nude mice to develop cohorts of tumor-bearing mice suitable for drug therapy in simulated early clinical trials. The xenografted tumors maintain their fundamental genotypic features despite serial passages and recapitulate the genetic heterogeneity of pancreatic cancer. The *in vivo* platform is useful for integrating drug screening with biomarker discovery. Passages of tumors in successive cohorts of mice do not change their susceptibility to anticancer agents and represent a perpetual live bank, facilitating the application of new technologies that will result in the creation of an integrated stable database of tumor-drug response data and biomarkers.

The majority of advanced solid malignancies in adults, including pancreatic cancer, are not curable with current conventional therapies (1). The introduction of targeted agents, such as inhibitors of the epidermal growth factor receptor (EGFR) and angiogenesis, has resulted in modest improvement in survival times in selected solid neoplasms (2–5). Targeted agents are most effective in neoplasms in which the pathway is important for the survival of the neoplasm and is effectively inhibited by treatment with the drug. The reason for the limited clinical success of most currently available agents is their failure to inhibit specific signaling pathways. Generalized clinical development strategies based on toxicity-based dose selection and "all comers" efficacy oriented testing have not been particularly productive. The development of EGFR inhibitors in lung cancer exemplified this issue. Whereas the overall activity of the drugs is limited, studies have now discovered the factors underlying susceptibility or resistance to these agents that will facilitate the implementation of enrichment strategies (6–9). These markers, however, have been discovered after thousands of patients have been treated with the drugs, many at the expense of high costs and toxicity events with no benefit. It is also likely that some other agents failed in the clinic because they were tested in unselected groups of patients and their potential beneficial effects were "diluted" by patients with no benefit. Furthermore, the failure of gefitinib, an inhibitor of the EGFR, to improve survival in lung cancer may have been in fact related to a selection of a dose too low to exert pharmacodynamic effects in carcinomas with wild-type receptor, suggesting that proper assays for dose selection and pharmacodynamic monitoring are critical.

Limited information on factors that are relevant to the efficacy of a drug at the time clinical trials are initiated is one of the underlying factors for the low yield rate in anticancer drug development. Before entering clinical development, agents are usually tested against high-passage commercially obtained cell lines and xenografts established from these lines. For cytotoxic agents, the activity against these xenografted neoplasms correlates with clinical activity to only a modest extent (10). Furthermore, all too often, no effort is placed on understanding why drugs may or may not work in these systems. Whereas these models are human in origin, they are in an artificial milieu and unlikely to fully recapitulate human cancers. Indeed, it is likely that the adaptation of neoplastic cells to *in vitro* conditions with successive passages for long periods has resulted in loss or gain

Authors' Affiliations: Departments of [1]Oncology, [2]Pathology, and [3]Surgery, Sidney Kimmel Comprehensive Cancer Center and the Sol Goldman Pancreatic Cancer Research Center at Johns Hopkins, The Johns Hopkins University School of Medicine, Baltimore, Maryland; [4]Response Genetics, Inc., Los Angeles, California; [5]Monogram Bioscience, Inc., South San Francisco, California; and [6]Department of Biochemistry and Molecular Biology, University of Southern California, Los Angeles, California

Received 1/17/06; revised 4/20/06; accepted 5/17/06.

Grant support: Goldman family, Lee family, the Viragh Foundation for Cancer Research, NIH grant CA113669 (A. Maitra and M. Hidalgo), and Specialized Program of Research Excellence in Gastrointestinal Cancer grant CA62924.

The costs of publication of this article were defrayed in part by the payment of page charges. This article must therefore be hereby marked *advertisement* in accordance with 18 U.S.C. Section 1734 solely to indicate this fact.

Note: Supplementary data for this article are available at Clinical Cancer Research Online (http://clincancerres.aacrjournals.org/).

Requests for reprints: Manuel Hidalgo, The Sidney Kimmel Comprehensive Cancer Center at Johns Hopkins, Room 1M89, 1650 Orleans Street, Baltimore, MD 21231. Phone: 410-502-3850; Fax: 410-614-9006; E-mail: mhidalg1@jhmi.edu.

doi:10.1158/1078-0432.CCR-06-0113

of genetic alterations that may be different from their parental tumors. This is illustrated, for example, by the studies of EGFR mutations that failed to identify in cell lines used in the preclinical development of these drugs the mutations that were found in primary carcinomas (7).

The purpose of this study was to develop, characterize, and test for major drug development–oriented applications an *in vivo* model using low-passage xenografts established directly from patients with pancreatic cancer. The goal was to develop well-defined cohorts of carcinomas, each one from a unique patient, which can be treated with new drugs as in human phase I-II clinical trials and used to address translational research questions. Here we present the results with 14 patient-derived carcinomas treated with four drugs, simulating the first stage of a classic human two-stage phase II clinical trial. Because the carcinomas are maintained *in vivo*, there is a continuous source of tissues for correlative studies before and after treatment using existing and novel technologies. The information gained can be added to an expanding database so that it can be transferred from one agent to another.

Materials and Methods

Tumor samples. Excess tissues from resected pancreatic carcinomas are routinely implanted in nude mice at the Johns Hopkins Medical Institutions to obtain highly pure neoplastic DNA under an Institutional Review Board–approved protocol (11). Briefly, excess tumor tissues not needed for clinical diagnosis from Whipple resection specimens are cut into 2- to 3-mm^3 pieces in antibiotic-containing RPMI medium. Pieces of nonnecrotic tissue are selected and immersed in Matrigel. Under anesthesia with isofluorane, tumors are implanted into 5- to 6-week-old female nu+/nu+ mice by a small incision and s.c. pocket made in each side of the lower back in which one tumor piece is deposited in each pocket. Tumors are harvested and stored for biological assays on reaching a size of 1,500 mm^3. From this set of xenografts, called F1, carcinomas from a total of 14 patients were obtained for subsequent expansion and drug treatment. None of these patients had undergone preoperative radiation therapy or preoperative chemotherapy.

Drugs. CI-1040, kindly provided as a gift from Pfizer (Ann Arbor, MI), was prepared in a vehicle of 10% cremophore EL (Sigma, St. Louis, MO), 10% DMSO, and 80% water. Temsirolimus (Wyeth Research, Colleville, PA) was dissolved in 10% ethanol, 10% pluronic, and 80% PBS. Erlotinib (OSI Pharmaceuticals, Melville, NY) was dissolved in 10% DMSO, 10% pluronic, and 80% PBS. Gemcitabine (Eli Lilly, Indianapolis, IN) was dissolved in saline. All drugs were freshly prepared and used at an injection volume of 0.2 mL/20 g body weight. Drug doses and treatment schedules were obtained from published studies.

Establishment of xenografts. Four- to six-week-old female athymic (nu/nu) mice were purchased from Harlan (Harlan Laboratories, Washington, DC). The research protocol was approved by the Johns Hopkins University Animal Use and Care Committee and animals were maintained in accordance to guidelines of the American Association of Laboratory Animal Care. Xenografts obtained from F1 mice were excised and cut into small ~3 × 3 × 3 mm fragments and then implanted s.c. in a group of five to six mice for each patient, with two small fragments in each mouse (F2) as described above for the original carcinoma. Half of the rest of the carcinoma was cryopreserved in liquid nitrogen and the other half is processed for biological studies. When the carcinoma reached a size of 1,500 mm^3, they were excised, cut into into ~3 × 3 × 3 mm fragments, and transplanted to the final cohort of mice that will be treated with the drugs (F3 and successive; Fig. 1).

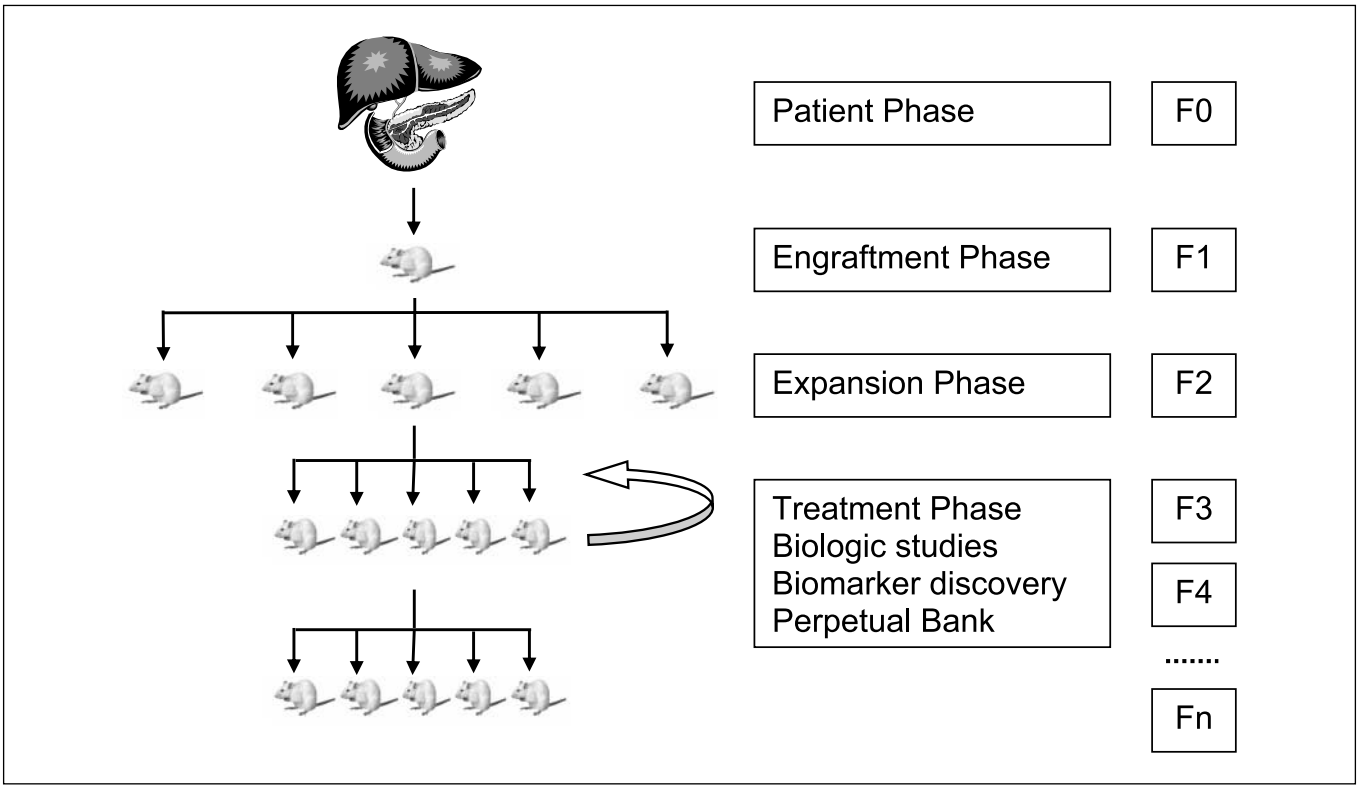

Fig. 1. Study schema. Tumor material is collected from residual tumor tissues at the time of Whipple resection and expanded in a cohort of nude mice using the procedure described in Materials and Methods.

Treatment protocol. Xenografts from this second mouse-to-mouse passage (F3) were allowed to grow to a size of ~200 mm^3, at which time mice were randomized in the following five groups of treatment, with six mice in each group: (*a*) control; (*b*) CI-1040 150 mg/kg/12 h i.p.; (*c*) erlotinib 50 mg/kg/d i.p.; (*d*) temsirolimus 20 mg/kg/d i.p.; and (*e*) gemcitabine 100 mg/kg twice a week i.p. Mice were treated during 28 days, monitored daily for signs of toxicity, and were weighed thrice a week. Tumor size was evaluated thrice a week by caliper measurements using the following formula: tumor volume = [length × $width^2$] / 2 as previously reported (12). Relative tumor growth inhibition (TGI) was calculated by relative tumor growth of treated mice divided by relative tumor growth of control mice (T/C). Experiments were terminated on day 28. We have defined a response as 0% to 20% TGI; stability, 21% to 50% TGI; and tumor progression, >50% TGI.

Mutation analysis. Genomic DNA was extracted from xenografts using DNeasy kit (Qiagen, Valencia, CA). Mutations of the *KRAS* gene were determined as previously described (13). PCR amplifications of exons 18, 19, and 21 of EGFR and exons 9, 10, and 20 of *PI3KCA* were done as described (7, 14, 15). *B-Raf* exons 11 and 15 and the full coding region for *mTOR* (exons 1-58) were amplified using the PCR-based techniques and a DNA amplification protocol established in our laboratory. The primers used are available on request. Briefly, 5 μL of each primer were added to give a concentration of 0.2 μmol/L along with 200 ng of genomic DNA to a 25-μL reaction mixture that consists of 12.5 μL HotMaster Mix 2.5× (Eppendorf, Westbury NY) containing 960 μmol/L deoxynucleotide triphosphates, 54 mmol/L KCl, 3.0 mmol/L $MgCl_2$, and 0.6 unit of Taq polymerase. The thermocycler conditions are as follows: an initial denaturation step of 94°C for 2 minutes, followed by 35 cycles of 94°C for 30 seconds, 55°C for 30 seconds and 68°C for 45 seconds followed by one cycle of 68° for 3 minutes. PCR product cleanup consists of 3 μL Shrimp alkaline phosphatase and 0.3 μL exonuclease 1 (GE Healthcare, Piscataway NJ) per sample, incubated at 37° for 1 hour, followed by one step of 80° for 15 minutes. The existence of the variant was determined by direct nucleotide sequencing in a cocktail consisting of 6 μL of PCR product at 3 ng per 100 bp of amplified product and 6 μL of either the forward or reverse primer at 1 μmol/L concentration. Sequencing in the forward and reverse direction was done using an ABI 3730XL Sequencer in the Genetics Resource Core Facility, Johns Hopkins University School of Medicine.

Immunohistochemistry. After harvesting, a representative sample of each xenograft was fixed in formalin for 24 hours and then embedded in paraffin. We constructed a tissue microarray in which each cancer specimen is represented by eight cores to obtain an adequate representation of tumor heterogeneity. For immunohistochemical studies, 0.5-μm sections of the tissue array were placed onto positively charged glass slides. Slides were deparaffinized and rehydrated in graded concentrations of alcohol by standard techniques before antigen retrieval in citrate buffer (pH 6.0) for 20 minutes. The slides were then cooled for 20 minutes before washing in 1× TBST (Dako Corp., Carpinteria, CA). All labeling was done using a DAKO Autostainer at room temperature. Slides were incubated in 3% H_2O_2 for 10 minutes, followed by the appropriate dilution of primary antibody for 60 minutes. Tris-HCl (0.2 mol/L, pH 7.5; Quality Biological, Inc., Gaithersburg, MD) was used as the antibody diluent solution. Negative controls were incubated for 60 minutes with the antibody diluent solution (0.2 mol/L Tris-HCl, pH 7.5; Quality Biological). Labeling was developed with the DAKO LSAB+ System (Dako) using the following conditions: biotinylated link for 10 minutes, streptavidin for 10 minutes, and substrate-chromagen (3,3′-diaminobenzidine) solution (DAKO Liquid DAB+ Substrate-Chromogen System) for 5 minutes. Slides were washed using 1× TBST after incubation with each reagent and with dH_2O following incubation with 3,3′-diaminobenzidine. Dpc4 labeling was done as reported (14). Dilutions of additional antibodies used were as follows: EGFR (clone 31G7, Zymed, San Francisco, CA), 1:50; p-EGFR (Calbiochem, San Diego, CA), 1:25; mitogen-activated protein kinase (MAPK; Cell Signaling), 1:25; pMAPK (Cell Signaling, Danvers, MA), 1:50; Akt (Santa Cruz Biotechnology, Inc.), 1:200; pAkt (Cell Signaling), 1:50; p70S6K (Santa Cruz Biotechnology, Santa Cruz, CA), 1:50; pp70S6K (Cell Signaling), 1:50; and dCK (generous gift from Dr. Iannis Talianidis; ref. 16). Immunohistochemical labeling of the neoplastic epithelium was done by one of the authors (C.I.-D.) who was blinded to the genotypic or phenotypic features of the xenografts, with negative labeling scored as 0 and positive labeling scored on a scale of 1+ to 3+, with 1+ corresponding to weak positive labeling, 2+ to unequivocal positive labeling, and 3+ to intense positive labeling.

Assessment of signaling-pathway activation by eTag method. A total of 16 frozen samples from four control and treated tumors in each of the treatment groups before and after treatment were used to determine activation of signaling the MAPK pathway. These studies were conducted by Monogram Biosciences, Inc. (South San Francisco, CA) using proprietary methods as published (17).

Fine-needle aspirate–based **ex vivo** *and pharmacodynamic studies.* Xenografts from three patients treated with CI-1040 (Panc 194, 198, and 215) were used for these studies. In the *ex vivo* experiments, each xenograft was sampled four times with a sterile 25-gauge short needle before the start of the treatment. Samples were immediately transferred into 10 mL of sterile, prewarmed complete RPMI 1640 containing 10% FCS, penicillin (200 μg/mL), and streptomycin (200 μg/mL). Cells were incubated with 0.04% trypan blue (Sigma) dissolved in PBS (9.1 mmol/L Na_2HPO_4, 1.7 mmol/L NaH_2PO4, and 150 mmol/L NaCl, pH 7.4). The viable (membrane-intact) and dead cells were then counted using Neubauer hemocytometer and the total viable cell count was used to calculate final working volumes. Approximately 75,000 tumor cells were seeded into each well of a six-well polypropylene microplate. Cells were treated in duplicate with vehicle (control) or CI-1040 in a humidified 5% CO_2 incubator at 37°C. Following treatment, non-adherent and adherent cells (collected by scraping) were pooled together in a 1.5-mL microcentrifuge tube and centrifuged at 500 × *g* for 5 minutes at 4°C. After washing with PBS, cells were lysed in 100 μL of ice-cold lysis buffer and analyzed on immunoblot. For the *in vivo* experiments, we obtained fine-needle aspirate (FNA) material, passing the needle through the xenograft 10 times with application of 1- to 2-mL suction. The aspirated material was expressed onto clear glass slides and smeared. All smears were allowed to air-dry and then stained with Diff-Quick stain (Baxter Healthcare, Miami, FL). Five to ten air-dried, Diff-Quick-stained cytologic smears were prepared from each tumor sample. The cellular composition of each aspirate was microscopically assessed by one of the authors (S.A.) under a microscope before protein extraction. FNA samples were collected from each animal before (day 0) and during (day 7) therapy. To prepare whole-cell lysates, the cells were collected from air-dried, Diff-Quick-stained slides by scraping into ice-cold buffer [50 mmol/L Tris-HCl, 0.25 mol/L NaCl, 0.1% (v/v) Triton ×100, 1 mmol/L EDTA, 50 mmol/L NaF, and 0.1 mmol/L Na_3VO_4, pH 7.4]. Protease inhibitors (protease inhibitor mixture, Roche Molecular Biochemicals, Mannheim, Germany) were added immediately. Cell lysates were centrifuged in an Eppendorf microcentrifuge (14,000 rpm, 5 minutes) at 4 °C and the supernatants were used in immunoblotting experiments.

Western blot analysis. Total cell lysates were obtained from either tumor cells from the *ex vivo* assays or from FNA samples. Protein extracts (15 μg) were added to a loading buffer [10 mmol/L Tris-HCl (pH 6.8), 1% SDS, 25% glycerol, 0.1 mmol/L mercaptoethanol, and 0.03% bromophenol blue], boiled, and electrophoresed on a 7% or 10% (w/v) polyacrylamide gel in the presence of SDS. Molecular weights of the immunoreactive proteins were estimated based on the relative migration with colored molecular weight protein markers (Amersham Pharmacia Biotech, Piscataway, NJ). After electrotransfer to Immobilon-P membranes (Millipore, Billerica, MA), membranes were blocked at room temperature using SuperBlock (Pierce, Rockford, IL) for 1 hour. The primary antibodies were diluted at 1:1,000 in 1:10 dilution of SuperBlock solution and the membranes were incubated with primary antibodies overnight at 4°C. The antibodies tested were p-Erk 1/2 (Cell Signaling) and total Erk 1/2 as well as proliferating cell

A

Patient	K-Ras	
	F0	F3
Panc 163	GAT/wt	GAT/wt
Panc 185	GAT/wt	GAT/wt
Panc 194	GTT/wt	GTT/wt
Panc 198	GAT/wt	GAT/wt
Panc 215	GAT/wt	GAT/wt
Panc 219	GAT/wt	GAT/wt
Panc 253	GAT/wt	GAT/wt
Panc 265	GAT/wt	GAT/wt
Panc 281	GTT/wt	GTT/GTT
Panc 286	GAT/wt	GAT/wt
Panc 287	wt/wt	wt/wt
Panc 294	GTT/wt	GTT/GTT

B

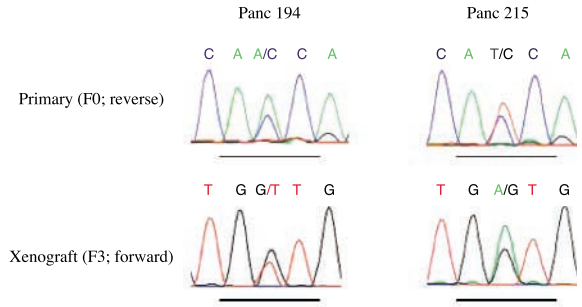

*Bracket indicates codon 12

Fig. 2. *KRAS* status in tumors. *A,* comparison of *KRAS* status in F0 and F3 tumors. Eleven of the 12 F0 carcinomas tested were *KRAS* gene mutant whereas one carcinoma was wild type. Exactly the same mutations were detected in 10 of the 12 F3 carcinomas. *B,* representative example of pair wild-type and mutant primary and xenografted tumor.

nuclear antigen (PC10; Santa Cruz Biotechnology). The next day, the membranes were washed and incubated for 1 hour at room temperature with horseradish peroxidase–conjugated secondary antibodies, rabbit immunoglobulin G-horseradish peroxidase or mouse immunoglobulin G-horseradish peroxidase (Santa Cruz Biotechnology), at a final dilution of 1:3,000. After washing thrice with TBS [10 mmol/L Tris-HCl (pH 7.5), 0.5 mol/L NaCl, and 0.05% (v/v) Tween 20], antibody binding was visualized using enhanced chemiluminescence (SuperSignal West Pico, Pierce) and autoradiography.

Reverse transcription-PCR. We determined the expression of a randomly selected set of genes in formalin-fixed, paraffin-embedded tissues in primary tumors (F0) and tumors from the F3 generation. Genes include nucleotide transporters (*NT*), cytidine deaminase (*CDA*), deoxycytidine kinase (*dCK*), dehydropyrimidine deshydrogenase (*DPD*), *EGFR*, nucleotide excision repair-1 (*ERCC-1*), folylpolyglutamate synthetase (*FPGS*), *HER2*, multidrug resistant protein 5 (*MRP5*), *p53*, nucleoside transporter 1 (*HENT1*), ribonucleotide reductase M1 and M2 subunits (*RRM1* and *RRM2*), thymidylate synthase (*TS*), and vascular endothelial growth factor (*VEGF*). These studies were done at Response Genetics, Inc. (Los Angeles, CA; refs. 18–25).

Statistical analysis. Data from individual experiments were averaged and presented as mean ± SD. The correlation between quantitative variables, including growth kinetics, biomarkers, and TGI, was assessed using the Pearson correlation coefficient. Tumors were classified as responses if the TGI was 0% to 20%, stable if the TGI was 21% to 50%, and resistant if TGI was >50%. Quantitative and categorical variables were compared between susceptible and resistant tumors using *t* test or χ^2 test, respectively.

Results

Model generation and kinetics. The general outline of the approach is depicted in Fig. 1. More than 80% of xenografted carcinomas engrafted satisfactorily in nude mice with a mean time to reach a size of 1,500 mm^3 of 7.6 ± 4.6 months. The "take" rate from F1 to F3 tumors was 93% with only one tumor failing to expand after successful engrafting in the mice. The proportion of tumors from each individual patient taking in the F2 generation was 70% to 100% and the mean time to reach a size of 200 mm^3 was 2.14 ± 0.79 months. In contrast, whereas the take rate from F2 to F3 generation was similar, the mean time to 200 mm^3 was 1 month shorter (1.3 ± 0.33 months). Overall, the data indicate that the model is feasible, efficient, and predictable.

Model stability. One important question is whether the process of engraftment and expansion in nude mice changes the genetic features of the tumors. To address this issue, we determined the mutation status of the *KRAS* gene and the expression of Dpc4 (Smad4) protein in paired F0 and F3 carcinomas. As shown in Fig. 2, 11 of the 12 F0 carcinomas tested were *KRAS* gene mutant whereas one carcinoma was wild type. Exactly the same mutations were detected in 10 of the 12 F3 carcinomas. Two carcinomas that were heterozygous in the F0 generation were found to be homozygously mutated in the F3 generation. This discrepancy may have been caused by allele dilution in the F0 carcinomas by DNA from residual nonneoplastic tissue. Dpc4 expression data are summarized in Fig. 3. We used Dpc4 immunohistochemistry because it has been shown to have an excellent correlation with gene status (14). Ten of 12 F0F3 pairs were concordant. One F0 carcinoma was heterogeneous with Dpc4-expressing and nonexpressing clones, but only an expressing clone was established in the xenograft. A second Dpc4-expressing carcinoma in the F0 material was found to be Dpc4 negative in the F3 generation. These data indicate a high degree of concordance between primary originator and xenografted carcinoma in this model.

A

Patient	DPC 4	
	F0	F3
Panc 163	+	+
Panc 185	-	-
Panc 194	-	-
Panc 198	-	-
Panc 215	+	+
Panc 219	+	+
Panc 253	+	+
Panc 265	Heterogeneous	+
Panc 281	-	-
Panc 286	+	+
Panc 287	-	-
Panc 294	+	-

B

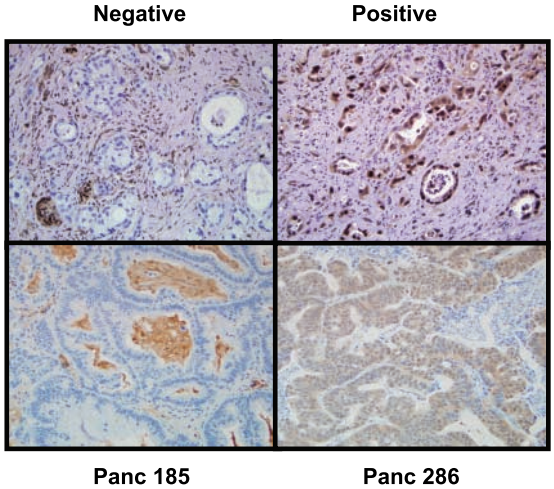

Fig. 3. Dpc4 status in tumors. *A,* comparison of immunolabeling for Dpc4 in F0 and F3 tumors. Ten of 12 F0-F3 pairs were identical showing the high degree of concordance between primary originator and xenografted carcinoma. *B,* representative pair comparison of Dpc4 immunohistochemistry in two primary pancreatic cancer xenografts and the corresponding xenografted tumors.

Table 1. Expression of selected genes in F0 and F3 tumors

Gene	Pearson correlation coefficient	*P*
NT	0.621289	0.215
CDA	0.729383	0.075
CDK	0.715542	0.089
DPD	0.714843	0.09
EGFR	0.461519	0.506
ERCC	0.671565	0.141
FGPS	0.667083	0.147
HER2	0.354965	0.696
MRP5	0.607454	0.237
p53	0.461519	0.506
HENT1	0.766159	0.054
RRM1	0.860814	0.006
RRM2	0.859069	0.006
TS	0.949737	0.001
VEGF	0.738918	0.066
Average	0.696276	0.189

We then measured the expression of 15 selected genes in paraffin-embedded tissues from the surgically resected primary carcinomas (F0) and their corresponding F3 xenografts. The data are summarized in Table 1. Overall, the coefficient of correlation was 0.69 (P = 0.1). Three genes (*TS*, *RRM1*, and *RRM2*) showed a statistically significant correlation (correlation coefficient, >0.8) whereas the other genes, such as *Her2*, *EGFR*, and *p53*, showed poor correlations (correlation coefficient, <0.5), indicating variability in gene expression between the primary carcinoma and the F3 xenograft.

In addition, because we plan to continue testing new agents against these carcinomas, we determined the TGI of three carcinomas after seven passages (F6 generation) to gemcitabine. As shown in Fig. 4, all carcinomas maintained their susceptibility/resistance status. In one carcinoma, however, the TGI increased from 51% to 85%.

Activity of selected anticancer agents. We studied the activity of gemcitabine and three targeted agents—erlotinib (EGFR inhibitor), temsirolimus (mTOR inhibitor), and CI-1040 (Erk inhibitor)—against this cohort of carcinomas. The number of carcinomas tested is similar to stage I of a two-stage phase II human clinical trial. Treatment responses are summarized in Table 2 and a representative tumor growth curve is shown in Fig. 5. The response rate ranged from 43% for gemcitabine to 0% for erlotinib. Interestingly, temsirolimus resulted in tumor stabilization in 12 carcinomas. No correlation was found between susceptibility to gemcitabine and susceptibility to signaling inhibitors. The activity of erlotinib correlated with that of CI-1040 (correlation coefficient, 0.74; P = 0.002) and

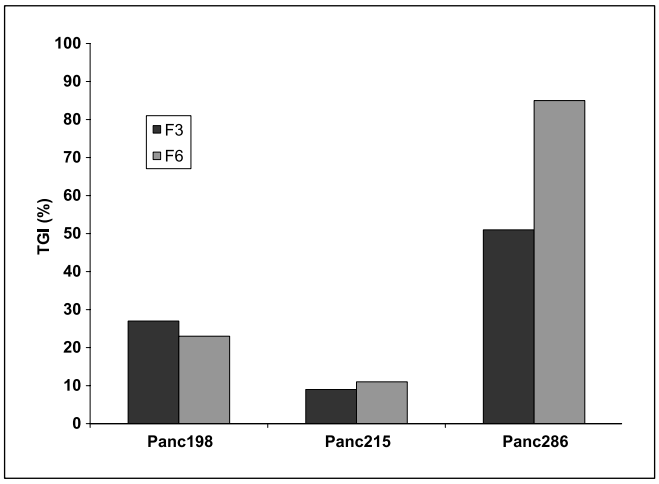

Fig. 4. TGI of gemcitabine in the F3 and F6 generation of three patient tumors. In subsequent passages, carcinomas maintained their susceptibility/resistance status to gemcitabine, showing the stability of this model.

there was statistically nonsignificant correlation between temsirolimus and CI-1040 ($R = 0.68$; $P = 0.1$).

Evaluation of predictors of response. One of the potential applications of this model is to study determinants of susceptibility to anticancer agents. The abundant neoplastic tissue permits using a variety of analytic techniques. To this end, we constructed a tissue microarray with these 14 carcinomas (Fig. 6A) using eight cores from F3 tumors. This strategy likely decreases the variability in markers measured in heterogeneous tumors. We measured the expression and activation of EGFR, MAPK, Akt, and p70S6K, using immunohistochemistry. In addition, we also determined expression of dCK and phosphatase and tensin homologue in these tumors. The results of these analyses are depicted in Fig. 6 and Supplementary Table S1A to C. For this analysis, we grouped tumors with TGI ≤50% as susceptible. There was a statistically significant association between the expression of EGFR and p-EGFR and the response to erlotinib. In addition, the carcinomas susceptible to this agent had higher levels of other EGFR signaling intermediaries, such as MAPK and Akt expression. Carcinomas susceptible to temsirolimus also had higher levels of p-EGFR and a trend towards higher p70S6K expression. Finally, p-EGFR was the only marker elevated in CI-1040-susceptible carcinomas, suggesting that carcinomas, depending on activation of the EGFR pathway, are more susceptible to inhibitors of either the receptor itself or the pathways that mediate the downstream effects of the receptor. Data about the expression of dCK, the enzyme involved in the intracellular activation of gemcitabine, are depicted in Fig. 6. Carcinomas with higher levels of the enzyme were more susceptible to the antitumor effects of the agent.

We also sought to sequence the key genes that are involved in the Ras/Raf/MAPK and phosphatidylinositol 3-kinase/Akt pathways. No mutations were found in the *EGFR TK, B-Raf, PI3K*, and *mTOR* genes. As expected, all but one carcinoma (Panc 287) were *KRAS* mutant. The *KRAS* wild-type tumor was resistant to erlotinib and CI-1040 but susceptible to temsirolimus. No differences in the immunohistochemistry profile were observed between this carcinoma and the *KRAS* gene mutant group.

Application of novel methods to predict antitumor efficacy. This set of studies was conducted to determine factors that may predict a response to targeted agents using novel methods. We selected CI-1040 as a representative agent to test these new methods. We determined pathway activation using eTag method, a technique that determines protein-protein interactions based on a proximity assay. We measured the

Table 2. Antitumor activity of selected anticancer agents

	Control	CI-1040 150 mg/kg Q 12 h	Erlotinib 50 mg/kg Q 24 h	Temsirolimus 20 mg/kg Q 24 h	Gemcitabine 100 mg/kg Twice a week
Efficacy [TGI (%)]					
Panc 159	100	20	52	43	3
Panc 163	100	57	61	47	33
Panc 185	100	45	62	30	20
Panc 194	100	78	88	82	25
Panc 198	100	17	29	20	20
Panc 215	100	83	90	41	9
Panc 219	100	57	63	47	64
Panc 253	100	69	66	45	9
Panc 265	100	35	84	30	19
Panc 266	100	51	62	37	32
Panc 281	100	45	62	42	22
Panc 286	100	37	58	30	51
Panc 287	100	54	67	37	28
Panc 294	100	51	59	50	14
Response		2 of 14	0 of 14	1 of 14	6 of 14
Rate (%)		14	0	7	43

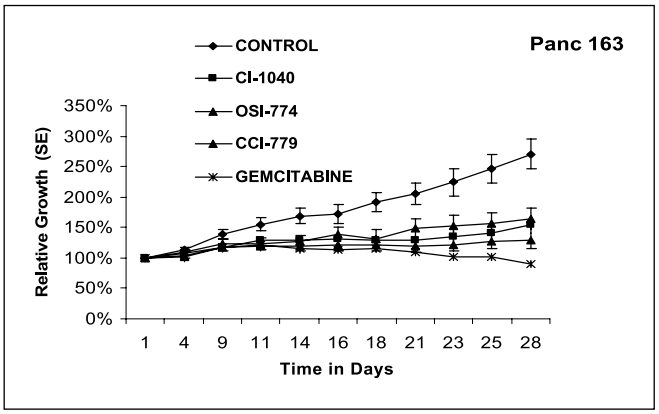

Fig. 5. Representative tumor growth curve of tumor Panc 163 treated with the studied agents. Drugs were administered at the dose and schedule described in Materials and Methods.

levels of expression of total and phosphorylated Erk before and 28 days after treatment with CI-1040. Each variable was measured in four representative samples from control and treated carcinomas for each of the 14 patient-derived carcinomas studied. Carcinomas susceptible to CI-1040 were characterized by statistically significant levels of activated Erk pathway. Levels of p-Erk/Erk were 111 in carcinomas susceptible to CI-1040 versus 37 in carcinomas resistant to the agent ($P = 0.03$; Fig. 7). In addition, whereas treatment with CI-1040 resulted in an average 37% inhibition in p-Erk in susceptible carcinomas, this variable increased by 19% in carcinomas resistant to the drug ($P = 0.02$). The combination of these two variables correctly predicted the susceptibility to CI-1040 in all the carcinomas.

We also explored whether *ex vivo* assays and pharmacodynamic monitoring applied to minimal tissue quantities could be used to predict tumor response. Figure 8 shows the results of this strategy applied to three carcinomas treated with CI-1040. Two of these carcinomas were resistant to the drug whereas one (Panc 198) was susceptible. In this technique, tumor samples were collected using FNA from tumors before treatment and exposed to CI-1040 *ex vivo*. As shown in Fig. 8, all three carcinomas expressed activated Erk that was inhibited by the agent *ex vivo* despite only one being susceptible. We next collected samples of these three carcinomas using FNA after 7 days of treatment. These studies, however, showed that CI-1040 failed to inhibit Erk activation in one of the resistant carcinomas. As expected, Panc 194, in which no target inhibition was shown, was resistant to CI-1040, indicating that target inhibition is a sine qua non for antitumor effects. Tumor 215, however, was resistant to treatment despite the target-inhibitory effects shown by the agent. Analysis of downstream markers of cell proliferation showed that the agent, despite inhibiting the target, failed to abort cell proliferation as shown by proliferating cell nuclear antigen labeling. In fact,

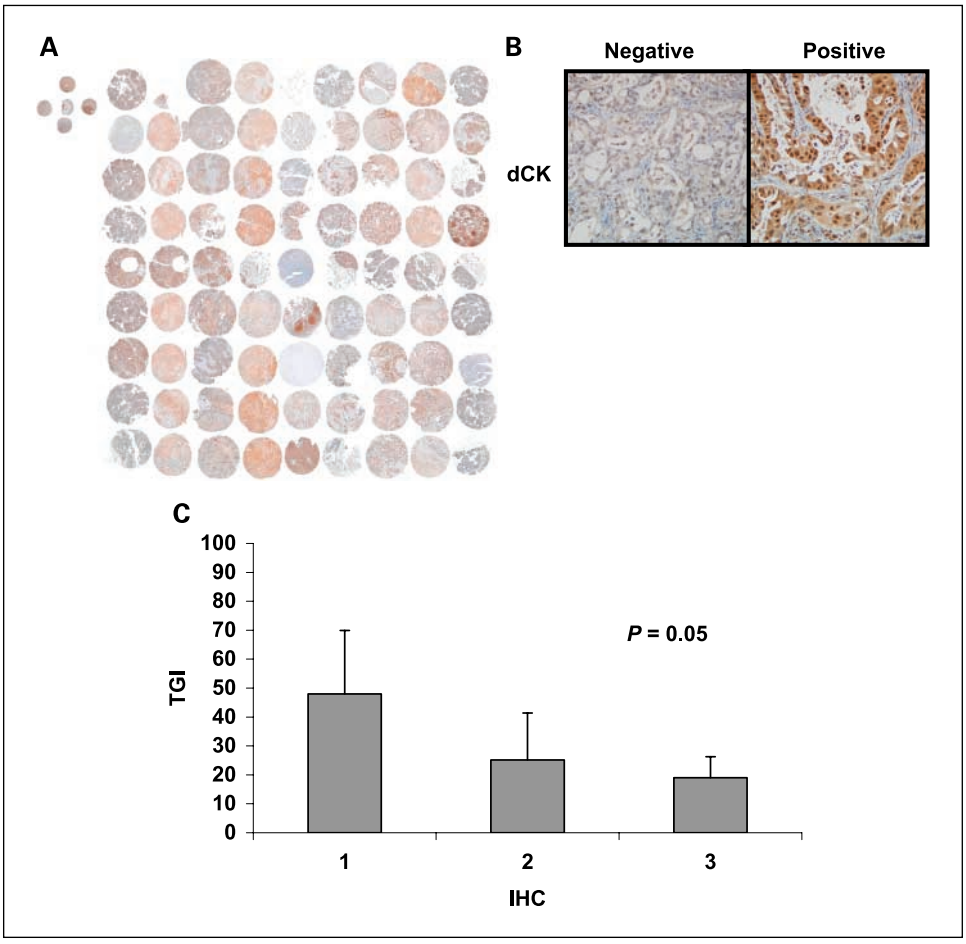

Fig. 6. *A,* panoramic view of tissue microarray immunolabeled for dCK. *B,* magnified view of two illustrative cases. *C,* TGI as a function of dCK immunohistochemistry score. Carcinomas with higher levels of the enzyme were more susceptible to the antitumor effects of the agent.

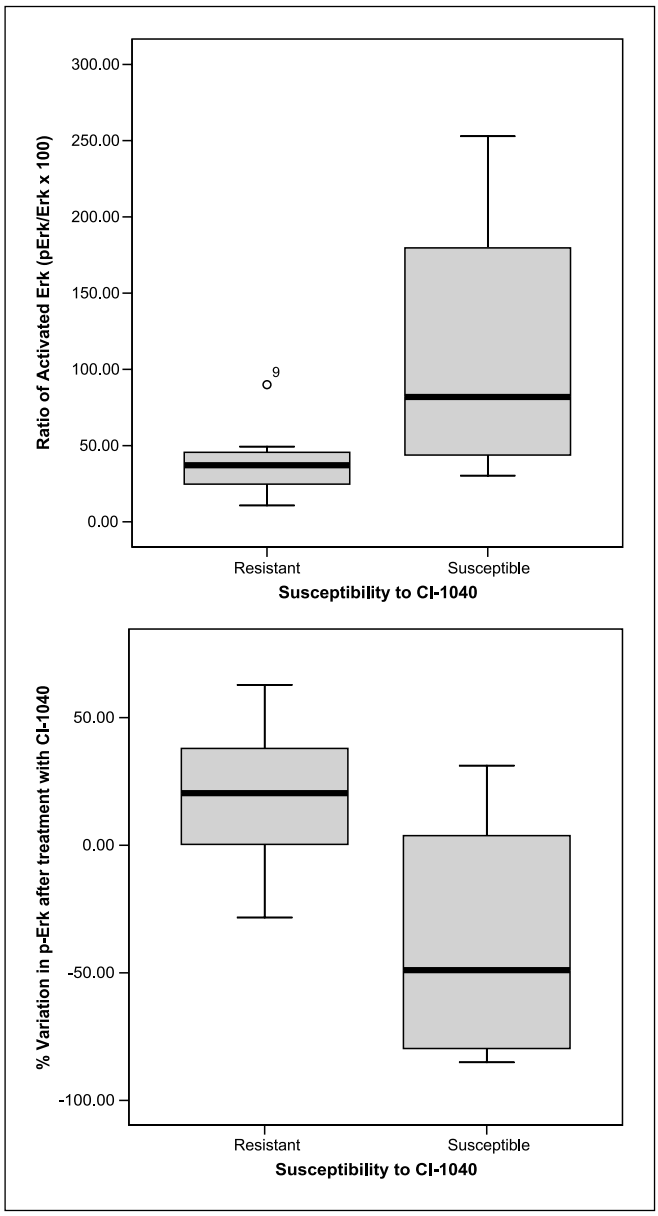

Fig. 7. Box plot depicting the ratio of p-Erk/Erk (*top*) and variations of the same (*bottom*) in tumors susceptible and resistant to CI-1040. Carcinomas susceptible to CI-1040 were characterized by activation of the Erk pathway and by its inhibition by the study drug.

downstream effects were only observed in Panc 198, a carcinoma that was susceptible to the agent. The data suggest that targeted agents will work only in tumors in which the target is present, in which the target is inhibited by the agent, and in which this inhibition effectively translates into downstream effects.

Discussion

The purpose of this study was to develop a clinically meaningful *in vivo* platform for late preclinical drug development in pancreatic cancer. Our goal was to establish a group of freshly generated xenografts that would allow us to conduct preclinical drug testing studies using methodologies similar to phase I and II human clinical trials. We believe this model has three major applications. First, it can be used as an *in vivo* screening modality to test novel drugs with therapeutic potential in pancreatic cancer. Second, the model is likely to be a rational platform to evaluate markers of response and resistance to drugs and to develop and apply novel technologies. Finally, this model may be used to select appropriate drugs to treat individual patients. The following paragraphs discuss the results of the studies from the perspective of these three applications.

First and foremost, our results show that this approach is feasible, at least in the context of pancreatic cancers. The take rate of the carcinoma is high and predictable and the growth kinetics in athymic mice are very homogeneous and similar to published studies (26–28). We waited until tumors in the F1 generation reached a size of 1,500 mm^3 before proceeding to F2 implants. This process took several months. We do not know if implanting F2 tumors earlier, before they reach 1,500 mm^3, is feasible. This strategy may be of interest because it can shorten the overall duration of the process, which may be of interest for its clinical applicability. Whether other types of cancers are also amenable to this approach remains to be determined. Smaller studies in colorectal cancer and lung cancer do indicate that this may be indeed feasible in other cancers as well (29–32). In addition, the study shows that drug testing is perfectly feasible in this model as is routinely done with conventional xenografted cell lines.

An important question is whether passaging of the carcinomas in the mice alters the genotype and phenotype of the neoplastic cells. This is important for at least two reasons. If there are fundamental changes in the carcinoma as they are generated and expanded in mice, the model may not reflect well the features of human pancreatic cancer and, therefore, the usefulness of this model as a screening platform for new drug development in this disease may be limited. Similarly, the value of this model as a "tool" to individualize patient treatment would be hampered. Our results show no major variations in the status of the principal genes mutated in pancreatic cancer, indicating that the fundamental pathogenetic elements remain stable. Indeed, the frequency of these genetic alterations is well within the expected frequency for pancreatic cancer, suggesting that these carcinomas are representative of pancreatic cancer as a whole. In contrast, the expression of a selected group of genes using reverse transcription-PCR methods showed variable results, with some genes showing a high degree of stability following serial xenografting and others not. It is not surprising that gene expression, which is a perturbable phenomenon, changes from F0 to F3 tumors. It should be noted, however, that we have tested a small sample size. Indeed, the correlation coefficients are >50% for most comparisons but did not reach statistical significance. In addition, we do not know if these changes translate into significant variations in protein expression, which is the most proximate determinant of drug response. It is important to emphasize that the relationship between gene expression and response to anticancer agents remains controversial for many drugs (22, 33–36). On the other hand, relatively stable genotypic alterations such as gene copy numbers and gene mutations seem to be more consistently linked to drug response (6, 37–39). Interestingly, we have compared the responses of the same pancreatic xenograft to gemcitabine across three generations (F3 and F6) and have

not observed any variations in therapeutic response, suggesting that, indeed, susceptibility or resistance is a stable trait.

An important consideration of this model, in contrast to existing preclinical models that use commercially available cell line resources, is that it will permit prospective clinical validation of preclinical efficacy data. We have undertaken this process using two complementary approaches. First, because almost all pancreatic cancer patients are treated in the clinic with gemcitabine either in the adjuvant or metastatic setting, we are in the process of initiating a clinical protocol to correlate the response of a patient's xenografted tumor to gemcitabine with the clinical outcome of the patient when treated with this agent. In addition, we are testing these carcinomas against a battery of different approved anticancer agents with the goal of prioritizing the agents that work best in the model to be used in the treatment of patients should their disease recur following treatment with gemcitabine. We expect that this study will validate the model as a predictor of clinical efficacy for anticancer agents. This approach is suitable in resected pancreatic cancer because patients are treated with adjuvant chemotherapy after resection and >80% develop disease progression with a median time to progression of 12 to 18 months, which is enough for engraftment of the carcinoma and testing of candidate drugs in the xenograft (40).

Targeted anticancer drugs are thought to work only in neoplasms in which the target is important and in which the target is properly inhibited by treatment with the agent. This hypothesis has been shown with kinase inhibitors at least and is the subject of significant attention and discussions (39, 41, 42). At the time most new drugs enter clinical development, this information is not known. We developed this model to help address this problem in pancreatic cancer. The model has the advantage that these carcinomas can be characterized in full detail for known drug targets using available methods. In addition, as new targets and analytic techniques become available, they can be easily incorporated. For example, we have determined the expression and activation of signaling pathways using conventional immunohistochemistry methods and have sequenced the genes that are more relevant in the activity of the agents tested in these studies. We have also applied a novel protein-protein interaction method and validated novel tissue acquisition procedures/assays, such as the FNA, for *ex vivo* assays and pharmacodynamic monitoring. Importantly, because the carcinomas are easily propagated in additional xenografts, analytic methods can be applied to multiple samples within the same tumor so that issues of cancer heterogeneity can be assessed. For example, the tissue microarray that we have built contains eight cores from each tumor, a sampling much larger than most of conventional tumor biopsies. The biological information obtained for each tumor is incorporated to a database and linked to drug response. This process will facilitate the elucidation of markers of drug response as well as the validation of new analytic methods. For example, CI-1040 is an Erk inhibitor and we show that the ratio of Erk activation in these carcinomas, as determined by eTag method, predicts outcome. CI-1040 has been clinically tested in an "all comers" clinical trials and showed activity in one patient with pancreatic cancer (43–45). The data from our study may lead to a focus clinical development of Erk inhibitors in patients with activation of the pathway. Furthermore, using FNA-guide pharmacodynamic monitoring, a procedure that can be easily incorporated into clinical trials, the data show that only carcinomas in which the targeted pathway and downstream effectors are inhibited by the drug respond to the agent. These data suggest that

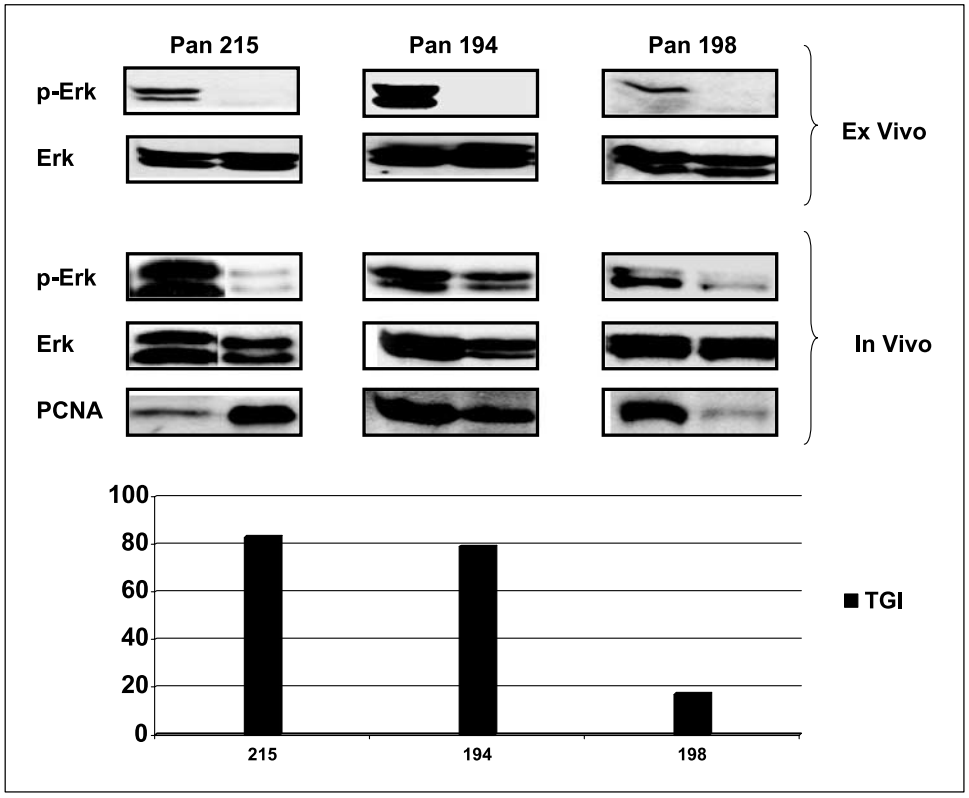

Fig. 8. CI-1040 inhibited Erk activation in FNA materials from three patient-tumors *ex vivo* (*top*) but only one was susceptible to drug as determined by TGI. In FNA collected on day 7 after treatment, the agent failed to inhibit Erk in one resistant tumor. Cell proliferation was inhibited only in the CI-1040-susceptible tumor.

pharmacodynamic monitoring may be needed to fully predict antitumor activity (Figs. 7 and 8). Overall, the data support the use of this model to develop and apply new methods for biomarker discovery with new anticancer agents.

In summary, we have developed a preclinical cancer model using freshly implanted pancreatic carcinomas. Carcinomas engrafted well and in a predictive manner with homogeneous kinetics. Whereas we have observed variations in gene expression, the significance of that finding is not known. The status of key genes in pancreatic cancer is, however, stable. Furthermore, there seems to be no changes in tumor response to anticancer agents with subsequent passages. The model can be used to apply, test, and validate established and novel methods to assess drug efficacy and pharmacodynamic effects. This model represents a new platform to explore new drugs in a mechanism-based fashion in pancreatic cancer.

References

1. Yeo TP, Hruban RH, Leach SD, et al. Pancreatic cancer. Curr Probl Cancer 2002;26:176–275.
2. Hurwitz H, Fehrenbacher L, Novotny W, et al. Bevacizumab plus irinotecan, fluorouracil, and leucovorin for metastatic colorectal cancer. N Engl J Med 2004; 350:2335–42.
3. Shepherd FA, Rodrigues Pereira J, Ciuleanu T, et al. Erlotinib in previously treated non-small-cell lung cancer. N Engl J Med 2005;353:123–32.
4. Tsao MS, Sakurada A, Cutz JC, et al. Erlotinib in lung cancer—molecular and clinical predictors of outcome. N Engl J Med 2005;353:133–44.
5. Moore M, Goldstein D, Hamm J, Figer A, et al. Erlotinib plus gemcitabine compared to gemcitabine alone in patients with advanced pancreatic cancer. A phase III trial of the National Cancer Institute of Canada Clinical Trials Group [NCIC-CTG]. Proc Asco 2005.
6. Paez JG, Janne PA, Lee JC, et al. EGFR mutations in lung cancer: correlation with clinical response to gefitinib therapy. Science 2004;304:1497–500.
7. Lynch TJ, Bell DW, Sordella R, et al. Activating mutations in the epidermal growth factor receptor underlying responsiveness of non-small-cell lung cancer to gefitinib. N Engl J Med 2004;350:2129–39.
8. Hirsch FR, Varella-Garcia M, McCoy J, et al. Increased epidermal growth factor receptor gene copy number detected by fluorescence *in situ* hybridization associates with increased sensitivity to gefitinib in patients with bronchioloalveolar carcinoma subtypes: a Southwest Oncology Group Study. J Clin Oncol 2005;23: 6838–45.
9. Moroni M, Veronese S, Benvenuti S, et al. Gene copy number for epidermal growth factor receptor (EGFR) and clinical response to antiEGFR treatment in colorectal cancer: a cohort study. Lancet Oncol 2005;6: 279–86.
10. Voskoglou-Nomikos T, Pater JL, Seymour L. Clinical predictive value of the *in vitro* cell line, human xenograft, and mouse allograft preclinical cancer models. Clin Cancer Res 2003;9:4227–39.
11. Walter K, Eshleman J, Goggins M. Xenografting and harvesting human ductal pancreatic adenocarcinomas for DNA analysis. Methods Mol Med 2005; 103:103–11.
12. Grunwald V, DeGraffenried L, Russel D, Friedrichs WE, Ray RB, Hidalgo M. Inhibitors of mTOR reverse doxorubicin resistance conferred by PTEN status in prostate cancer cells. Cancer Res 2002;62:6141–5.
13. Shi C, Eshleman SH, Jones D, et al. LigAmp for sensitive detection of single-nucleotide differences. Nat Methods 2004;1:141–7.
14. Embuscado EE, Laheru D, Ricci F, et al. Immortalizing the complexity of cancer metastasis: genetic features of lethal metastatic pancreatic cancer obtained from rapid autopsy. Cancer Biol Ther 2005;4:548–54.
15. Samuels Y, Wang Z, Bardelli A, et al. High frequency of mutations of the PIK3CA gene in human cancers. Science 2004;304:554.
16. Hatzis P, Al-Madhoon AS, Jullig M, Petrakis TG, Eriksson S, Talianidis I. The intracellular localization of deoxycytidine kinase. J Biol Chem 1998;273: 30239–43.
17. Chan-Hui PY, Stephens K, Warnock RA, Singh S. Applications of eTag trade mark assay platform to systems biology approaches in molecular oncology and toxicology studies. Clin Immunol 2004;111:162–74.
18. Kakimoto M, Uetake H, Osanai T, et al. Thymidylate synthase and dihydropyrimidine dehydrogenase gene expression in breast cancer predicts 5-FU sensitivity by a histocultural drug sensitivity test. Cancer Lett 2005;223:103–11.
19. Cappuzzo F, Hirsch FR, Rossi E, et al. Epidermal growth factor receptor gene and protein and gefitinib sensitivity in non-small-cell lung cancer. J Natl Cancer Inst 2005;97:643–55.
20. Joshi MB, Shirota Y, Danenberg KD, et al. High gene expression of TS1, GSTP1, and ERCC1 are risk factors for survival in patients treated with trimodality therapy for esophageal cancer. Clin Cancer Res 2005; 11: 2215–21.
21. Schneider S, Uchida K, Brabender J, et al. Downregulation of TS, DPD, ERCC1, GST-Pi EGFR, HER2 gene expression after neoadjuvant three-modality treatment in patients with esophageal cancer. J Am Coll Surg 2005;200:336–44.
22. Rosell R, Danenberg KD, Alberola V, et al. Ribonucleotide reductase messenger RNA expression and survival in gemcitabine/cisplatin-treated advanced non-small cell lung cancer patients. Clin Cancer Res 2004;10:1318–25.
23. Lord RV, Park JM, Wickramasinghe K, et al. Vascular endothelial growth factor and basic fibroblast growth factor expression in esophageal adenocarcinoma and Barrett esophagus. J Thorac Cardiovasc Surg 2003; 125:246–53.
24. Salonga DS, Danenberg KD, Grem J, Park JM, Danenberg PV. Relative gene expression in normal and tumor tissue by quantitative RT-PCR. Methods Mol Biol 2002;191:83–98.
25. Lenz HJ, Danenberg KD, Leichman CG, et al. p53 and thymidylate synthase expression in untreated stage II colon cancer: associations with recurrence, survival, and site. Clin Cancer Res 1998;4: 1227–34.
26. Bocsi J, Zalatnai A. Establishment and long-term xenografting of human pancreatic carcinomas in immunosuppressed mice: changes and stability in morphology, DNA ploidy and proliferation activity. J Cancer Res Clin Oncol 1999;125:9–19.
27. Reyes G, Villanueva A, Garcia C, et al. Orthotopic xenografts of human pancreatic carcinomas acquire genetic aberrations during dissemination in nude mice. Cancer Res 1996;56:5713–9.
28. Sorio C, Bonora A, Orlandini S, et al. Successful xenografting of cryopreserved primary pancreatic cancers. Virchows Arch 2001;438:154–8.
29. Perez-Soler R, Kemp B, Wu QP, et al. Response and determinants of sensitivity to paclitaxel in human non-small cell lung cancer tumors heterotransplanted in nude mice. Clin Cancer Res 2000;6:4932–8.
30. Giovanella BC, Vardeman DM, Williams LJ, et al. Heterotransplantation of human breast carcinomas in nude mice. Correlation between successful heterotransplants, poor prognosis and amplification of the HER-2/neu oncogene. Int J Cancer 1991;47:66–71.
31. Elkas JC, Baldwin RL, Pegram M, Tseng Y, Slamon D, Karlan BY. A human ovarian carcinoma murine xenograft model useful for preclinical trials. Gynecol Oncol 2002;87:200–6.
32. Fichtner I, Slisow W, Gill J, et al. Anticancer drug response and expression of molecular markers in early-passage xenotransplanted colon carcinomas. Eur J Cancer 2004;40:298–307.
33. Kroep JR, Loves WJ, van der Wilt CL, et al. Pretreatment deoxycytidine kinase levels predict *in vivo* gemcitabine sensitivity. Mol Cancer Ther 2002;1:371–6.
34. Kornmann M, Schwabe W, Sander S, et al. Thymidylate synthase and dihydropyrimidine dehydrogenase mRNA expression levels: predictors for survival in colorectal cancer patients receiving adjuvant 5-fluorouracil. Clin Cancer Res 2003;9:4116–24.
35. Westra JL, Hollema H, Schaapveld M, et al. Predictive value of thymidylate synthase and dihydropyrimidine dehydrogenase protein expression on survival in adjuvantly treated stage III colon cancer patients. Ann Oncol 2005;16:1646–53.
36. Inoue T, Hibi K, Nakayama G, et al. Expression level of thymidylate synthase is a good predictor of chemosensitivity to 5-fluorouracil in colorectal cancer. J Gastroenterol 2005;40:143–7.
37. Pegram MD, Pauletti G, Slamon DJ. HER-2/neu as a predictive marker of response to breast cancer therapy. Breast Cancer Res Treat 1998;52:65–77.
38. Sawyers CL. Opportunities and challenges in the development of kinase inhibitor therapy for cancer. Genes Dev 2003;17:2998–3010.
39. Sawyers C. Targeted cancer therapy. Nature 2004; 432:294–7.
40. Yeo CJ. The recent past and future of adjuvant therapy for pancreatic cancer. Ann Surg Oncol 2003;10: 488–9.
41. Arteaga CL, Baselga J. Tyrosine kinase inhibitors: why does the current process of clinical development not apply to them? Cancer Cell 2004;5:525–31.
42. Baselga J, Arribas J. Treating cancer's kinase "addiction." Nat Med 2004;10:786–7.
43. Adjei AA, Hidalgo M. Treating cancer by blocking cell signals. J Clin Oncol 2005;23:5279–80.
44. Lorusso PM, Adjei AA, Varterasian M, et al. Phase I and pharmacodynamic study of the oral MEK inhibitor CI-1040 in patients with advanced malignancies. J Clin Oncol 2005;23:5281–93.
45. Rinehart J, Adjei AA, Lorusso PM, et al. Multicenter phase IIstudy of the oral MEK inhibitor, CI-1040, in patients with advanced non-small-cell lung, breast, colon, and pancreatic cancer. J Clin Oncol 2004;22: 4456–62.